Time-Resolved Emission Spectra of Fluoroprobe and Maleimido-Fluoroprobe before, during, and after Sudden Vitrification of Radiation-Polymerized Methyl Methacrylate

Mark S. Frahn,* Leonard H. Luthjens, and John M. Warman

Radiation Chemistry Department, IRI, Delft University of Technology, Mekelweg 15, 2629 JB Delft, The Netherlands

Received: September 4, 2003

We have monitored in situ the changes that occur in the charge-transfer (CT) emission from the highly fluorescent probe molecule Fluoroprobe (FP) and its fluorogenic derivative Maleimido-Fluoroprobe (MFP) during the radiation-induced polymerization of methyl methacrylate (MMA). While FP remains as a free, fluorescent molecule in the polymerizing medium, MFP is nonfluorescent and displays FP-like fluorescence only when the maleimido group is incorporated into a growing polymer chain to form its copolymerized, succinimido derivative (pMFP). Very abrupt and pronounced changes in both the spectrum and decay kinetics of the fluorescence are found for both probe molecules on traversing the narrow dose region of the gel effect in which the medium suddenly changes from a slightly viscous liquid to a rigid polymeric glass. The two probe molecules display close to identical behavior, apart from a slight indication of preferential concentration of pMFP in polymer-rich and FP in monomer-rich regions of the medium just prior to vitrification. The in situ CT fluorescence spectra and decay kinetics in the fully polymerized PMMA matrix are characteristic of a slightly polar medium with a dielectric constant close to the static value of 3.5 for PMMA. More detailed (ex situ), wavelength-dependent kinetic studies of fully polymerized samples show a bathochromic shift in the fluorescence to occur with a spectral relaxation time of 16 ns for both probe molecules. This is orders of magnitude shorter than the shortest dielectric relaxation time measured in AC studies and is attributed to rapid reorganization of the dipolar side-chain ester groups of the polymer induced by the fully charged donor and acceptor centers in the CT state of the FP chromophore.

Introduction

In the present study, we have monitored the fluorescence of the probe molecules 1-phenyl-4-[(4-cyano-1-naphthyl)methylene]piperidine, hereafter named Fluoroprobe (FP), and the fluorogenic derivative 1-*p*-maleimido-phenyl-4-[(4-cyano-1-naphthyl)methylene]piperidine, hereafter named Maleimido-Fluoroprobe (MFP) during the course of radiation-induced polymerization of bulk methyl methacrylate (MMA). The chemical structures of both probe molecules are given in Figure 1. Of interest was a comparison between the behavior of the free fluorophore (FP) with that of a derivative that only fluoresces when copolymerized (MFP). Previous studies have shown how the latter, fluorogenic probe molecule can be used to monitor the progress of polymerization even in the early stages of polymerization where the viscoelastic properties of the medium differ little from those of the starting material.[1−3] MFP has also the unique fluorogenic property that makes it possible to monitor polymerization in dilute solution as well as in the bulk monomer.[4] In this paper we focus more on the changes occurring in the region of the "gel" or Trommsdorff effect where sudden vitrification occurs. Particular attention is paid to the information that can be gained concerning the microscopic nature of the ultimate, glassy PMMA matrix.

When the carbon−carbon double bond of the maleimido group in MFP becomes saturated, this nonfluorescent molecule exhibits strong charge-transfer (CT) fluorescence similar to that of FP. Because of the exceptional sensitivity of their fluorescence to specific material properties such as polarity, polarizability, and viscosity, both of these probes have been extensively investigated.[2,3,5−8,9−13] This sensitivity is attributed to the formation of a large dipole moment in the excited state following photoexcitation.[7] This large dipole moment is a consequence of electron transfer from the donor, dialkylanilino group to the cyano-naphthylmethylene acceptor.

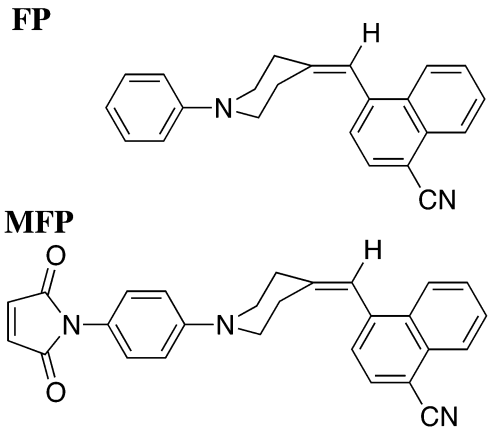

Figure 1. Molecular structures of the fluorescent (FP) and fluorogenic (MFP) probe molecules used in the present work.

Figure 2 illustrates the consequences of solvent relaxation on the CT fluorescence. After electron transfer occurs, dipolar solvent molecules reorient around the molecule, predominately by rotation, thus stabilizing the excited state. Femtosecond time-resolved fluorescence measurements and molecular dynamics

* Author to whom correspondence may be addrssed. E-mail: MSFrahn@Netscape.net. Tel: +31-6-4840-8388. Fax: +31-15-278-7421.

10.1021/jp0366419 CCC: $27.50
Published on Web 02/05/2004

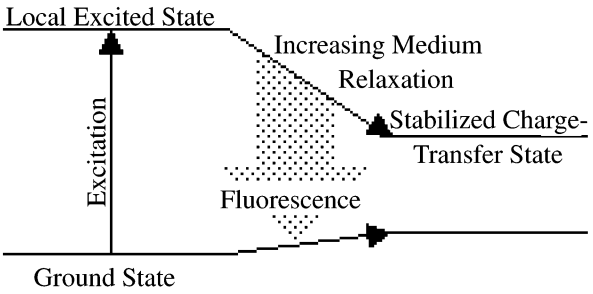

Figure 2. A schematic representation of the photoexcitation of a donor−spacer−acceptor molecule such as Fluoroprobe illustrating the decrease in energy of the emission from the highly dipolar, charge-separated state that results from reorganization of the dipoles in the surrounding medium.

calculations on FP have established that this stabilization occurs in low viscosity solvents within a time scale of a few picoseconds.[11−13] The extent of stabilization is strongly dependent on the polarity of the solvent. For this reason, increasingly redshifted fluorescence is observed in solvents of increasing polarity.

The solvatochromic power of the present probe molecules can be demonstrated by constructing Lippert−Mataga plots in which the wavenumber of the fluorescence maximum, υ_{CT}, is plotted against the solvent polarity parameter Δf. This parameter is related to the static dielectric constant ϵ_s and the optical refractive index n, as shown in eq 1

$$\Delta f = (\epsilon_s - 1)/(2\epsilon_s + 1) - (n^2 - 1)/(2n^2 + 1) \qquad (1)$$

The Lippert−Mataga equation,[14,15] derived by assuming the ground-state dipole moment to be negligible in comparison to that in the emissive CT state, is given below

$$\upsilon_{CT} = \upsilon_{CT}(0) - 1.007 \times 10^4[(\mu_{CT})^2/\rho^3]\Delta f \qquad (2)$$

In eq 2, $\upsilon_{CT}(0)$ (cm^{-1}) is the wavenumber corresponding to the (hypothetical) gas-phase fluorescence maximum, μ_{CT} is the dipole moment of the CT state in Debye, and ρ is the effective radius in Å of a spherical cavity containing the molecule (frequently taken to be 40% of the long axis for elongated molecules such as FP[7]). A plot of υ_{CT} vs Δf for FP has the exceptionally large slope of $-34\,000$ cm^{-1} from which a dipole moment of the CT state of ca. 25 D, corresponding to complete charge separation, is determined. This large dipole moment has been confirmed by time-resolved microwave conductivity measurements.[7]

Additional photophysical characteristics of FP are presented in Table 1 together with the frequently used solvent polarity parameter $E_T(30)$.[16] The dependencies of the photon energy at the maximum of the emission, E_{max}, and the fluorescence lifetime, τ_{FL}, on the solvent polarity parameter are shown in Figure 3. As expected from the previous discussion, E_{max} decreases continuously with increasing solvent polarity. The dependence of τ_{FL} on polarity is however seen to be more complex, passing through a maximum at intermediate polarities. The decrease in lifetime on the high-polarity side of the maximum is attributed to the decrease in energy between the CT state and the ground state which results in an increased rate of charge recombination according to the Marcus expression for the inverted region.[17] The decrease in lifetime on the low-polarity side is attributed to mixing between the CT state and the locally excited state of the acceptor which results in an additional pathway to the ground state.[10,18]

TABLE 1: Photophysical Properties of Fluoroprobe in Various Solvents

solvent[a]	$E_T(30)$[b]	λ_{max} (nm)	E_{max} (eV)	τ_{FL} (ns)
cyclohexane	31.2	412	3.01	1.2
di-*n*-butyl ether	33.4	468	2.65	12
benzene	34.5	478	2.59	15
diethyl ether	34.6	506	2.45	14
1,4-dioxane	36.0	516	2.40	15
tetrahydrofuran	37.4	574	2.16	7.0
ethyl acetate	38.1	573	2.16	6.0
1,2-dimethoxyethane	38.2	595	2.08	4.0
pyridine	40.2	627	1.98	1.0
MMA		550	2.25	9.0
PMMA		450	2.75	11[c]

[a] Reference 7. [b] Reference 16. [c] Long-time decay component (when fit using a biexponential decay model).

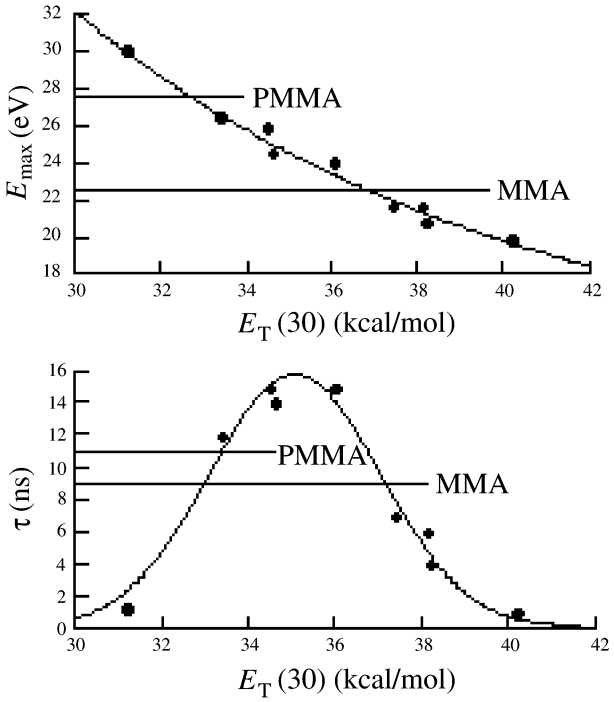

Figure 3. The dependence of the maximum energy (upper figure) and the decay time (lower figure) of Fluoroprobe emission on the polarity parameter $E_T(30)$ for the solvents listed in Tabel 1. The horizontal lines correspond to the values of E_{max} and τ found for MMA and PMMA.

As mentioned previously, relaxation of solvent molecules around the excited-state dipole of FP will occur within a few picoseconds in fluid media, i.e., on a time scale much shorter than the nanosecond lifetime of the excited state. The emission can therefore be taken to be from the fully matrix-equilibrated CT state. However, when imbedded in a highly viscous medium, the time-scale on which reorientation of dipoles occurs can approach, or even exceed, that of the fluorescence lifetime. Such an occurrence is experimentally detectable as a bathochromic shift of the fluorescence with time. This effect has previously been demonstrated for FP in glass-forming solvents by thermochromic studies involving streak camera measurements.[9] A method of analyzing such time-resolved emission spectra (TRES) has been presented by Lakowicz.[19] This treatment will be discussed in more detail and applied to the present measurements in the Results and Discussion section.

Experimental Section

Materials. Methyl methacrylate (Merck, Synthesis grade) was deaerated and distilled on a vacuum line at atmospheric pressure

and 100−101 °C immediately prior to use. The probe molecules FP[7,20] and MFP[21] were synthesized in the group of Prof. J. W. Verhoeven of the Department of Organic Chemistry at the University of Amsterdam (for molecular structures, see Figure 1). Dilute solutions in MMA of ca. 10^{-4} molar were prepared and pipetted into sample cells constructed (in-house) of Heraeus Suprasil, 1 cm square, quartz tubing with an attachment that allowed the solutions to be dearated by three freeze−pump−thaw cycles on a vacuum line.

Methods. Optical absorption spectra of the solutions were measured using a Perkin-Elmer Lambda 40 UV/VIS spectrophotometer. The optical densities at the excitation wavelength of 337 nm used in fluorescence measurements were 0.5 or 2 for the 1-cm path length of the cells used. Steady-state fluorescence spectra of irradiated samples could be measured outside of the radiation chamber using a Photon technology International "Quantamaster 1" spectrofluorimeter.

In situ measurements of the fluorescence spectra, carried out within the irradiation chamber during the course of polymerization, were achieved using an experimental setup which has been described in detail previously.[1] The excitation wavelength was ca. 340 nm, and emission spectra were recorded using a diode array spectrophotometer (Ocean Optics Europe S2000). Spectra could be obtained at time intervals as short as 2 s.

In situ fluorescence decay measurements were obtained using an experimental flash-photolysis setup described in detail in a separate publication.[22] The samples were photoexcited with a ca. 500-ps duration pulse of 337-nm light from a Lasertechnik Berlin MSG 800 laser. The integrated emission above 350 nm was detected using a silicon semiconductor photodiode with rise and fall times of ca. 1 ns (EG&G FWD-100Q). The output of the detector was monitored and stored using a 1 GHz digital oscilloscope (Tektronix TDS 680B).

Wavelength-dependent, time-resolved fluorescence decay measurements on fully polymerized samples were made outside the gamma irradiator using a nitrogen laser (Laser Photonics MegaPlus LN 1000), which produces pulses of 337-nm radiation with a pulse width at half height of ca. 800 ps. The excitation light is incident on the sample at an angle of 90° to the detection system. Emitted light is focused onto a monochromator (American ISA Incorporated H-20 SA) with variable entrance and exit slits. In this way, the bandwidth could be varied from 2 to 8 nm. The emitted light is detected using a single channel-plate photomultiplier (Photek PMT 113/UHF Ultrafast MCP Photomultiplier) with ca. 100-ps rise and fall times. The output of the detector is monitored by a real-time, 1-GHz digital oscilloscope (Tektronix TDS 680B). Data acquisition and handling was accomplished with the LabVIEW Package (version 5.1) from National Instruments Corporation.

γ-Ray irradiations at ca. 8 kGy/hr were accomplished with an MDS Nordion cobalt-60 Gammacell 220 irradiator. Dose rates were accurately determined by Fricke dosimetry and corrected for the natural decay of the source. The ambient temperature within the source chamber was 33 °C.

Results and Discussion

In this section, we present results on the changes which occur in the spectrum and decay kinetics of the fluorescence from dilute solutions of FP and MFP in MMA during the course of radiation-induced polymerization. We focus particularly on the range of radiation dose within which the gel effect occurs. The application of MFP and other fluorogenic probe molecules to quantitatively monitor the degree of monomer conversion at lower doses and in dilute solution has been demonstrated in previous publications.[1−4,22−24]

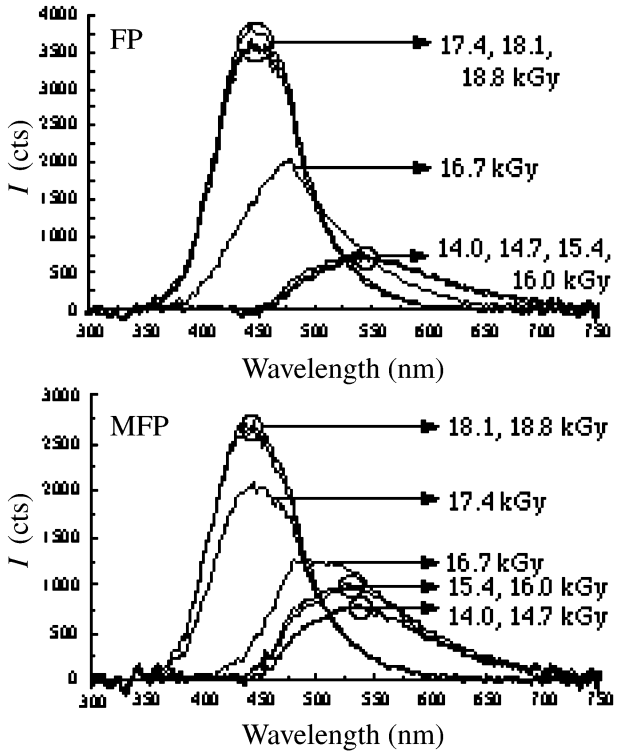

Figure 4. Fluorescence spectra measured in situ during radiation-induced polymerization of MMA containing Fluoroprobe (upper) and Maleimido-Fluoroprobe (lower). The data are show for radiation doses just prior to, during, and just after the occurrence of the gel effect and the sudden virtrification of the medium.

An aspect of interest in the present study was whether different fluorescent behavior would be observed in the gel region between that from "free" FP molecules and that from the FP chromophoric units of copolymerized MFP, "pMFP", which are pendantly bound to polymer chains[2]. It was thought that if phase separation occurred during vitrification, then FP might be preferentially concentrated in low molecular weight, *monomer-rich* regions whereas pMFP would emit mainly from *polymer-rich* regions. By comparison of the two probe molecules therefore, we hoped to be able to obtain more detailed information on the morphological changes occurring on a microscopic scale during the course of autoacceleration and vitrification.

Fluorescence Spectra, in situ Measurements. Fluorescence spectra of MMA solutions of FP and MFP measured in situ for radiation doses in the vicinity of the gel effect are shown in Figure 4. For both solutes, an abrupt blueshift in the emission maximum, from ca. 550 nm (2.25 eV) to ca. 450 nm (2.75 eV) occurs within the dose range between 15 and 17 kGy. The wavelength shift is very similar to that found on thermal curing of MMA containing FP.[5] Also, as expected, it agrees with that found previously in this laboratory in an experimental procedure which required the samples to be removed from the radiation source and measured using an external spectrofluorimeter.[1] The present, in situ measurement capability was designed in order to make it possible to take spectra at more frequent time intervals during the gel effect and to eliminate postirradiation effects during sample transport between the source and the spectrofluorimeter. The spectra shown in Figure 4 were taken at 5-min intervals after a prior irradiation for a period of ca. 2 h.

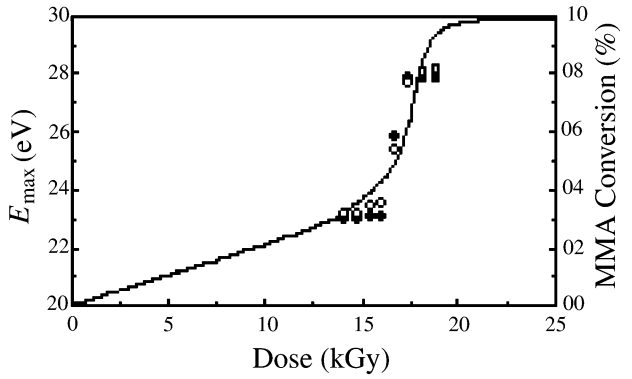

Figure 5. The dependence of the maximum energy of the emission, E_{max}, on radiation dose in the region of the occurrence of the gel effect for MMA containing FP (○) and MFP (□). Also shown is the monomer conversion under the same radiolysis conditions.

The energy maxima of the spectra in Figure 4 are plotted as a function of radiation dose in Figure 5. Also shown in the figure is the MMA monomer conversion measured under the same dose-rate conditions. The response of the two probe molecules during the course of vitrification is seen to be very similar. MFP does however display evidence of a gradual blueshift prior to vitrification which is absent for FP. In fact, for FP, only one of the spectra within a 5-min time span differs significantly from that of the two extremes. This is thought to reflect the different tendencies of the pMFP and FP fluorophores to be concentrated mainly in polymer-rich or monomer-rich regions of the medium, respectively. The close to discontinuous change found for FP indicates therefore that polymerization within the monomer-rich regions must eventually occur *extremely* rapidly.

Comparison of the E_{max} values prior to and after the gel effect with the data in Figure 3 for the emission from solvents of different polarity indicates that the effective polarity parameter, $E_T(30)$, changes from 37 to 33. The latter value, for the fully polymerized PMMA matrix, is still higher than the value of ca. 31 found for a completely nonpolar (hydrocarbon) medium. It is, in fact, close to the value found for the weakly polar solvent di-*n*-butyl ether, which has a dielectric constant of 3.08. Since the room-temperature dielectric constant of PMMA is 3.45, it would appear that a large fraction of the dipolar relaxation potential of the PMMA matrix is involved in reducing the energy level of the CT state of FP and pMFP, even within the excited-state lifetime of a few nanoseconds. This will be discussed in more detail after first considering the time-resolved measurements of the fluorescence decay kinetics.

Fluorescence Decay, in situ Measurements. In addition to the sudden hypsochromic shift in the emission maximum on vitrification, there is also an abrupt change in the decay kinetics of the fluorescence for both probe molecules. The decay of the integrated fluorescence for FP, measured in situ, is shown in parts A and B of Figure 6. For radiation doses just prior to the gel effect, the decay is monoexponential with a mean decay time of 9.0 ns. On vitrification however the decay deviates considerably from monoexponential at early times. A best biexponential fit to the data, given by the full line in Figure 6B, was found for lifetime components $\tau_1 \approx 3.0$ and $\tau_2 \approx 11$ ns. The values of τ_1 and τ_2 determined from best fits for both FP and MFP are plotted against dose in Figure 7. As with the spectral shifts, the change in decay kinetics is also seen to occur over an extremely narrow range of dose and no substantial difference is found between the two probe molecules.

Comparison of the major, long-lifetime component of 11 ns for the fully polymerized medium with the lifetimes found for

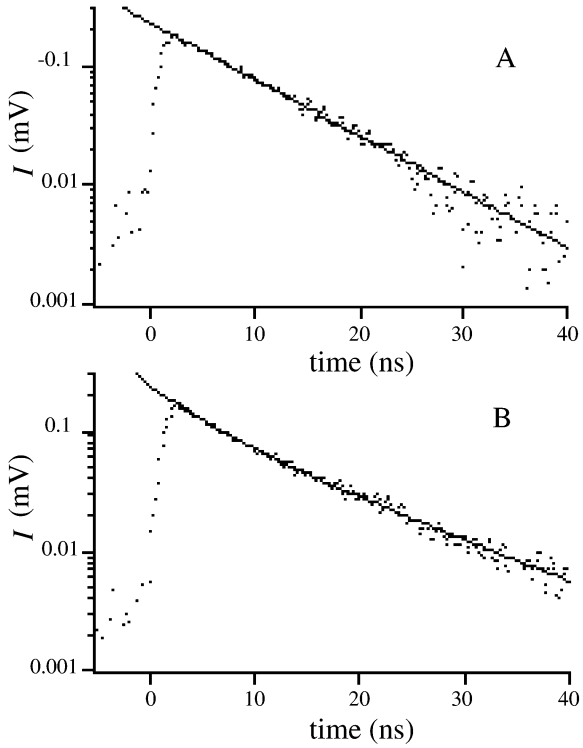

Figure 6. Integrated fluorescence transients measured in situ on laser flash photolysis (800 ps, 355 nm pulse) of MMA containing Fluoroprobe (A) just prior to the gel effect, dose = 14.0 kGy, and (B) just after the gel effect, dose = 18.8 kGy. The full lines are fits to the after-pulse decay of fluorescence using (A) a single exponential with a mean lifetime of 9.0 ns and (B) a biexponential with lifetime components of 3.0 and 11 ns.

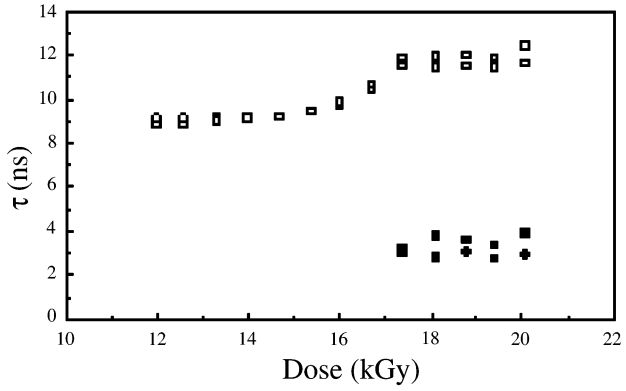

Figure 7. The short (filled symbols) and long (open symbols) lifetime components determined from biexponential fits to the fluorescence decay for radiation doses in the region of the occurrence of the gel effect for MMA containing FP (circles) and MFP (squares).

solvents of different polarities indicates that the effective E_T-(30) value is close to 33 for PMMA, in agreement with the conclusion reached on the basis of the emission maximum. The spectral and kinetic data are therefore consistent. To investigate further the underlying cause of the nonexponential decay of the integrated fluorescence in the polymerized medium found in the in situ measurements, more detailed experiments have been carried out on fully polymerized samples that were removed from the radiation source and investigated using time-resolved fluorescence equipment capable of monitoring fluorescence transients at specific wavelengths. These measurements are reported in the next subsection.

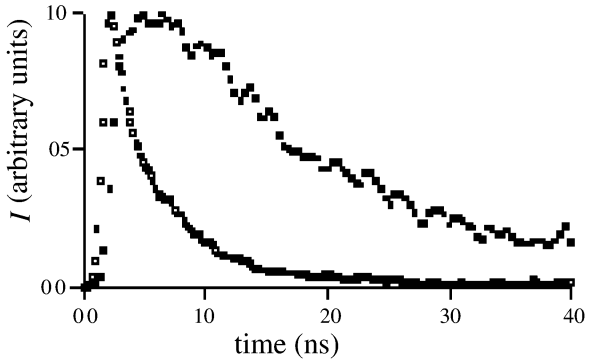

Figure 8. Fluorescence transients monitored at 380 and 580 nm on laser flash photolysis of a fully polymerized PMMA sample containing Fluoroprobe illustrating the rapid decay at the short wavelength extreme of the emission and the after-pulse growth at the long wavelength extreme.

Fluorescence Decay Kinetics in PMMA, Wavelength Dependence. The two most common underlying causes of the nonexponential decay of the integrated fluorescence in solid matrixes can be separated into "static" and "dynamic" effects. In the static case, the fluorescent molecules are considered to be entrapped within a variety of local dielectric or structural environments, each resulting in a different spectrum and/or decay time of the fluorophore emission. In the dynamic case, changes in the emissive properties are brought about by relaxation of the local environment or the structure of the fluorophore itself on a time scale similar to that of the mean lifetime of the fluorescent state. Molecules with highly dipolar excited states, as in the present work, are expected to be particularly susceptible to both static and dynamic effects.

In the case of static effects, the fluorescence may display different decay times at different wavelengths, hence, resulting in an overall nonexponential decay of the integrated fluorescence. However, the decay at all individual wavelengths will be continuous and monoexponential. In the case of dynamic effects, which are invariably expected to result in a gradual decrease in the energy of the emission, a decay in the short wavelength region is expected to be accompanied by a *growth* at long wavelengths.

In Figure 8 fluorescence transients are shown, which were taken at the blue and red extremes of the fluorescence spectrum found in the in situ experiments, at 380 and 580 nm, respectively. The decay at 380 nm is seen to be much faster than at 580 nm, with a lifetime close to the value of 3 ns found for the short component in the in situ measurements. More importantly, the fluorescence at 580 nm is seen to grow in over the first few nanoseconds after the pulse. This growth, over a post-pulse period of approximately 5 ns, is much slower than would be expected on the basis of the ca. 200-ps response time of the equipment. This presents therefore clear-cut evidence that dynamic changes in the local environment or structure of the fluorophores are the underlying cause of the nonexponential decay of the integrated fluorescence.

To more fully investigate the relaxation process involved requires constructing time-resolved emission spectra that will be discussed in the following subsection.

Time-Resolved Emission Spectra (TRES). TRES can be measured directly, e.g., by pulse sampling with time-gated detection, or can be constructed from the wavelength-dependent decays together with the steady-state emission spectrum. The latter procedure involves fitting the decays $I(\lambda,t)$ with the following multiexponential relationship[19]

$$I(\lambda,t) = \sum_i \alpha_i(\lambda)\exp[-t/\tau_i(\lambda)] \quad (3)$$

In eq 3, $\tau_i(l)$ and $\alpha_i(\lambda)$ are wavelength-dependent decay times and pre-exponential factors (with $\sum\alpha_i = 1$). Because of parameter correlation and limited resolution, no molecular significance can be assigned to these parameters. A set of parameters $H(\lambda)$ is then determined in which the intensity decays are normalized to the steady-state emission spectrum $F(\lambda)$

$$H(\lambda) = F(\lambda)/\int I(\lambda,t)\,dt \quad (4)$$

which for multiexponential analysis becomes

$$H(\lambda) = F(\lambda)/\sum_i \alpha_i(\lambda)\tau_i(\lambda) \quad (5)$$

The normalized intensity decay functions $I'(\lambda,t)$ are then given by

$$I'(\lambda,t) = H(\lambda)I(\lambda,t) = \sum_i \alpha'_i(\lambda)\exp[-t/\tau_i(\lambda)] \quad (6)$$

in which $\alpha'_i(\lambda) = H(\lambda)\alpha_i(\lambda)$. These appropriately normalized decays are then used to construct the TRES.

By use of this procedure, TRES were calculated for both FP and MFP in PMMA. For this purpose, external measurements of both the decay profiles and steady-state emission spectra were made. Figure 9 shows the peak-normalized TRES for both FP and MFP. The spectra given in the figure were calculated at time intervals of 2.5 ns. The left-most TRES corresponds to a time of 2.5 ns following the excitation pulse, and the right-most TRES corresponds to a time of 40 ns. The data are similar for both solutes, apart from what would appear to be a larger spectral shift at early times for MFP.

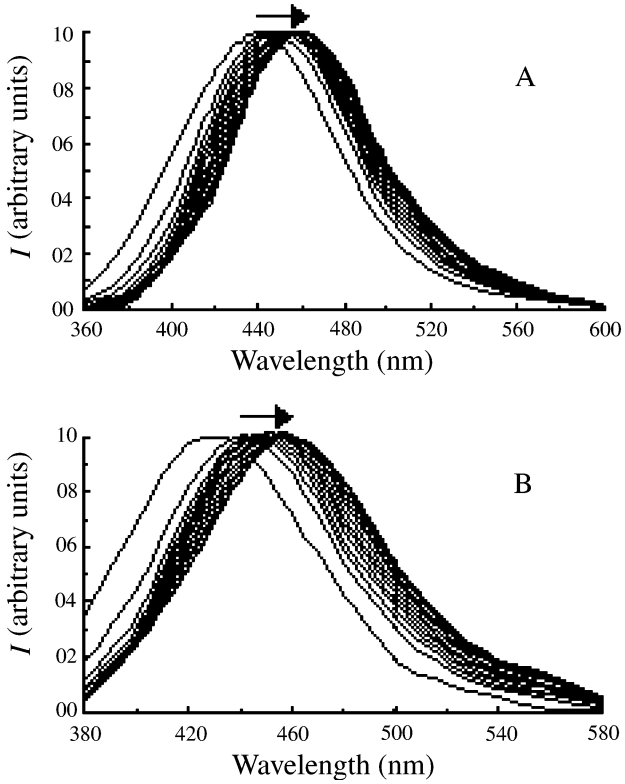

Figure 9. Peak-normalized TRES for PMMA samples containing FP (A) and MFP (B). The spectra, which are for time intervals of 2.5 ns within a total elapsed time of 40 ns after the pulse, show a gradual spectral shift to longer wavelengths with time.

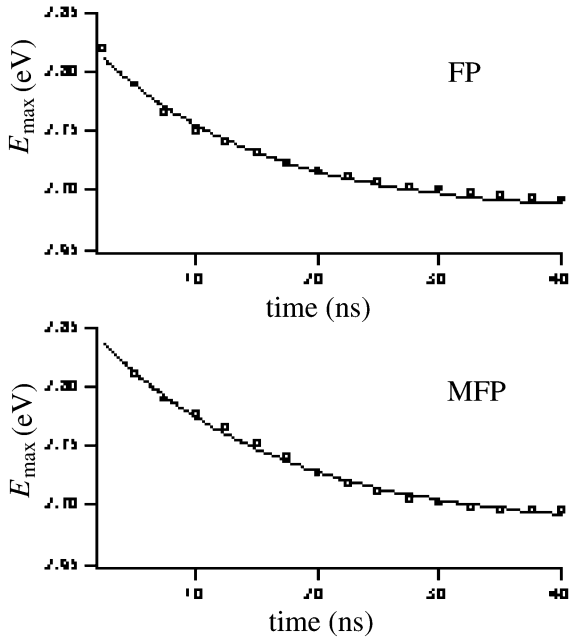

Figure 10. The time dependence of the maximum of the TRES shown in Figure 9 (○). The full lines correspond to a monoexponential relaxation of E_{max} to an eventual constant value of 2.68 eV with a relaxation time of 16 ns.

In Figure 10 the values of E_{max} are plotted as a function of time. Apart from the initial rapid decrease for MFP mentioned above, the decrease in energy is seen to display a closely similar temporal behavior for both solutes. The full lines in the figure were calculated on the basis of an exponential relaxation to a long-time limiting value of $E_{max} = 2.68$ eV, with a relaxation time of 16 ns.

The overall shift in E_{max} from 2.83 eV (438 nm) to 2.68 eV (462 nm) is very close to the 20-nm shift over a time span of 100 ns reported by van Ramesdonk et al. for FP in thermally polymerized MMA.[5] Ramesdonk et al. argued that the source of the spectral relaxation on a nanosecond time scale must be due to conformational rearrangement of the fluorophore rather than relaxation of the PMMA matrix. This was based on the fact that dielectric relaxation of PMMA has been found to occur on a time scale orders of magnitude longer than that for relaxation of the FP emission.[25−27] The intramolecular conformational change was ascribed to "rehybridization of the amino nitrogen into a planar trigonal situation". We consider that the identical values for the fluorescence relaxation time found for FP and MFP argue against this interpretation. In the case of pMFP, the anilino group is coupled, via the copolymerized maleimido moiety, to the polymer chains. This added restriction to the motional freedom would be expected to have a considerable retarding effect on the kinetics of planarization about the anilino nitrogen and hence result in a slower relaxation time than for the free FP molecules. The lack of a difference in relaxation kinetics leads us to conclude that the underlying cause of relaxation must indeed be reorganization of the PMMA matrix, probably involving side-chain motions of neighboring ester groups. As mentioned above, the time scale of fluorescence relaxation is orders of magnitude shorter than the dielectric relaxation time attributed to such motions. We conclude that the Coulombic interaction between the fully charged donor and acceptor moieties in the excited state of the present fluorophores and neighboring dipolar ester groups is sufficiently strong to overcome the barrier to structural reorganization.

Because all experiments were conducted at a temperature above the β-relaxation transition of PMMA,[28] the molecular origin of the stabilization interaction is tentatively attributed to side-chain motions of the PMMA ester groups. This is perhaps counterintuitive when one considers the time scale attributed to such relaxations in PMMA.[25,29,27,26,5] Nevertheless, the large dipole moment of ca. 25 ± 2 D produced upon charge separation in the excited state is highly probable to exert a significant Coulombic force on nearby ester groups in the matrix thus providing a pathway for matrix reorganization within the nanosecond time scale.

Conclusions

In situ measurements have been made of the spectra and decay kinetics of the charge-transfer fluorescence of the fluorescent and fluorogenic probe molecules FP and MFP during the course of radiation-induced polymerization of MMA in a cobalt γ-ray source. Particular attention has been paid to the range of radiation dose in which the gel effect, resulting in sudden vitrification, occurs. This effect results in an abrupt blueshift in the fluorescence maximum from ca. 550 to 450 nm for both compounds with a slight indication of a previtrification shift for MFP but not for FP. This difference in behavior is attributed to the preferential concentration in polymer-rich and monomer-rich regions of the sample, respectively. The spectral change is accompanied by a change in the decay kinetics from monoexponential with a decay time of 9.0 ns to non-monoexponential, with a biexponential fit yielding lifetime components of ca. 3 and 11 ns. Both the spectral shift and the change in the (long) lifetime correspond to a change in the $E_T(30)$ polarity parameter of the medium from 37 prior to to 33 after the gel effect. The latter value, for the fully polymerized matrix, corresponds to that found for the weakly polar solvent di-*n*-butyl ether, which has a dielectric constant of 3.08, close to the static dielectric constant of PMMA. A wavelength-dependent study of the fluorescence decay in fully polymerized samples, conducted outside of the source, has been used to construct TRES. The TRES display a gradual redshift in the emission maximum that occurs with an exponential relaxation time of 16 ns. This is attributed to reorganization of the dipolar side-chain esther groups of the polymer induced by the highly dipolar, fully charge-separated state of the probe molecules, on a time scale orders of magnitude shorter than the dielectric relaxation time of PMMA. No evidence is found for (micro)-heterogeneity in the PMMA matrix.

Acknowledgment. The authors thank professor J.W. Verhoeven (University of Amsterdam) for providing the Fluoroprobe and Maleimido-Fluoroprobe compounds used in this work.

References and Notes

(1) Warman, J.; Abellon, R.; Luthjens, L.; Suykerbuyk, J.; Verhey, H.; Verhoeven, J. *Nucl. Instrum. Methods Phys. Res., Sect. B* **1999**, *151*, 361.

(2) Warman, J. M.; Abellon, R. D.; Verhey, H. J.; Verhoeven, J. W.; Hofstraat, J. W. *J. Phys. Chem. B* **1997**, *101*, 4913.

(3) Frahn, M. S.; Abellon, R. D.; Luthjens, L. H.; Warman, J. M. *Radiat. Res. Proc.* **1999**, *2*, 86.

(4) Frahn, M. S.; Luthjens, L. H.; Warman, J. M. Submitted 2003.

(5) van Ramesdonk, H.; Vos, M.; Verhoeven, J.; Möhlmann, G.; Tissink, N.; Meesen, A. *Polymer* **1987**, *28*, 951.

(6) Jenneskens, L.; Verhey, H.; van Ramesdonk, H.; Witteveen, A.; Verhoeven, J. *Macromolecules* **1991**, *24*, 4038.

(7) Mes, G. F.; Jong, B. d.; van Ramesdonk, H. J.; Verhoeven, J. W.; Warman, J. M.; Haas, M. P. d.; Horsman-van den Dool, L. E. W. *J. Am. Chem. Soc.* **1984**, *106*, 6524.

(8) Hofstraat, J.; Verhey, H.; Verhoeven, J.; Kumke, M.; Li, G.; Hemmingsen, S.; McGrown, L. *Polymer* **1997**, *38*, 2899.
(9) Goes, M.; Groot, M. d.; Koeberg, M.; Verhoeven, J. W.; Lokan, N. R.; Shephard, M. J.; Paddon-Row: M. N. *J. Phys. Chem. A* **2002**, *106*, 2129.
(10) Pasman, P.; Rob, F.; Verhoeven, J. W. *J. Am. Chem. Soc.* **1982**, *104*, 5127.
(11) Middelhoek, E. R.; Vermeulen, P.; Verhoeven, J. W.; Glasbeek, M. *Chem. Phys. Lett.* **1995**, *198*, 373.
(12) Middelhoek, E. R.; Zhang, H.; Verhoeven, J. W.; Glasbeek, M. *Chem. Phys.* **1996**, *211*, 489.
(13) Brown, R.; Middelhoek, R.; Glasbeek, M. *J. Phys. Chem.* **1999**, *111*, 3616.
(14) Lippert, E. Z. *Naturforsch.* **1955**, *10a*, 541.
(15) Mataga, N. *Bull. Chem. Soc. Jpn.* **1955**, *28*, 690.
(16) Reichardt, C. *Solvent Effects in Organic Chemistry*; Weinheim: New York, 1979; Vol. 3
(17) Marcus, R. A. *Annu. Rev. Phys. Chem.* **1964**, *15*, 155.
(18) Depaemelaere, S.; Viaene, L.; Auweraer, M. v. d.; Schryver, F. C. D.; Hermant, R. M.; Verhoeven, J. W. *Chem. Phys. Lett.* **1993**, 215.
(19) Lakowicz, J. R. *Principles of Fluorescence Spectroscopy*, 2nd ed.; Kluwer Academic/Plenum Press: New York, 1999.
(20) Hermant, R. M. Ph.D. Thesis, University of Amsterdam, 1990.
(21) Verhey, H. V.; Bekker, C. H. W.; Verhoeven, J. W.; Hofstraat, J. W. *New J. Chem.* **1996**, *20*, 809.
(22) Frahn, M. S.; Abellon, R. D.; Luthjens, L. H.; Vermeulen, M. J. W.; Warman, J. M. In press.
(23) Frahn, M. S.; Abellon, R. D.; Jager, W. F.; Luthjens, L. H.; Warman, J. M. *Nucl. Instrum. Methods Phys. Res., Sect. B* **2001**, *185*, 241.
(24) Frahn, M. S.; Warman, J. M.; Abellon, R. D.; Luthjens, L. H. *Radiat. Phys. Chem.* **2001**, *60*, 433.
(25) Deutsch, K.; Hoff, E. A.; Reddish, W. *J. Polym. Sci.* **1954**, *13*, 565.
(26) McCrum, N. G.; Read, B. E.; Williams, G. *Anelastic and Dielectric Effects in Polymeric Solids*; John Wiley & Sons Ltd.: London, 1967.
(27) Smyth, C. P. *Physics and Chemistry of the Organic Solid State*; Interscience: New York, 1963; Vol. 1.
(28) Ward, I. M.; Hadley, D. W. *An Introduction to the Mechanical Properties of Solid Polymers*; John Wiley & Sons Ltd: Chichester, 1928.
(29) Sinnot, K. M. *J. Polym. Sci.* **1960**, *42*, 3.